Electronic Supplementary Material (ESI) for Soft Matter.
This journal is © The Royal Society of Chemistry 2021

Cluster and conquer: The morphodynamics of invasion of a compliant substrate by active rods

Mohammad Imaran[1,2,3], Mandar M Inamdar[4],

Ranganathan Prabhakar[2], Raghunath Chelakkot[31]

[11] *IITB-Monash Research Academy, Mumbai, India*

[2] *Department of Mechanical & Aerospace Engineering,*

Monash University, Clayton, Australia

[3] *Department of Physics, Indian Institute of Technology Bombay, Mumbai, India*

[4] *Department of Civil Engineering, Indian Institute of Technology Bombay, Mumbai, India*

I. MODEL EQUATIONS

The two-dimensional system consists of $N_{\rm r}$ active rods and $N_{\rm s}$ substrate particles. Each active rod is modeled as a *rigid* linear array of $N_{\rm b}$ "beads" of equal mass, m_b. Each bead has a nominal diameter, $\sigma_{\rm b}$.

The length of the rod , $L = N_{\rm b}\,\sigma_{\rm b}$ and its mass, $m_r = N_b\,m_b$. The centre-of-mass of the i-th rod, $\mathbf{r}_i$ and the instantaneous unit vector defining its orientation, $\mathbf{p}_i$ evolve according to the following equations of motion:

$$\frac{d\,\mathbf{r}_i}{d\,t} = \mathbf{v}_i\,, \tag{1}$$

$$\frac{d\,\mathbf{p}_i}{d\,t} = \boldsymbol{\omega}_i\,, \tag{2}$$

$$m_r\,\frac{d\,\mathbf{v}_i}{d\,t} = \mathbf{F}_i^{\rm tot}\,, \tag{3}$$

$$I_r\,\frac{d\,\boldsymbol{\omega}_i}{d\,t} = \mathbf{T}_i^{\rm tot}\,, \tag{4}$$

where I_r is the moment of inertia of a rod about its centre, and $\mathbf{v}_i$ and $\boldsymbol{\omega}_i$ are its centre-of-mass velocity and the angular rotation rate about its centre, respectively.

The differential equations above are integrated forward by the LAMMPS **fix rigid/nve** package with a time-step of size Δt after determining the forces and torques on the right-hand side. The positions of the individual beads comprising the rigid rods and their velocities are updated using rigid-body kinematics.

There are five different forces that act on the ν-th bead in the i-th rod: the active propulsive force, excluded-volume repulsion from beads of neighbouring rods, excluded-volume repulsion from substrate particles, frictional resistance from the substrate, and random noise.

- A propulsion force of magnitude $F^{\rm a}$ is distributed equally on all beads of each rod and acts along the instantaneous rod axis, $\hat{\mathbf{p}}_i$. Hence, the propulsion force on any bead of the rod , $\mathbf{F}^{\rm a}_{\nu,\,i} = \left(F^{\rm a}/N_{\rm b}\right)\hat{\mathbf{p}}_i$.

- Each bead on a rod interacts with beads on other neighbouring through the Separation, Shifted Lennard-Jones (SSLJ) excluded-volume potential [1], described further below.

- The excluded-volume repulsion between a bead and neigbouring substrate particles is similarly modeled.

- In the context of bacteria moving through furrows in a plastic substrate, such as agar, the furrows contain an aqueous fluid. The bare frictional force on a bead when the rod moves through such "empty" furrows is $\mathbf{F}^{\mathrm{f}}_{\nu,i} = -\gamma_b \mathbf{v}_{\nu,i}$, where γ_b is a constant friction coefficient. Frictional interactions between beads of rods is neglected.

- The components of the random force on each bead, $\mathbf{F}^{\mathrm{r}}_{\nu,i}$, are independent Gaussian random numbers such that:

$$\left\langle \mathbf{F}^{\mathrm{r}}_{\nu,i}(t) \right\rangle = \mathbf{0}\,; \tag{5}$$

$$\left\langle \mathbf{F}^{\mathrm{r}}_{\nu,i}(t)\, \mathbf{F}_{\mu,j}(t') \right\rangle = 2\,\gamma_b\, k_B\, T\, \Delta t\, \delta(t-t')\, \delta_{ij}\, \delta_{\mu\nu}\, \boldsymbol{\delta}\,, \tag{6}$$

  where δ is the Dirac delta-function, δ_{pq} is the Kronecker-delta functions, and $\boldsymbol{\delta}$ is the isotropic tensor, k_{B} is the Boltzmann constant and T is the absolute temperature.

Then, the total force on the ν-th bead of the i-th rod is

$$\mathbf{F}_{\nu,i} = \mathbf{F}^{\mathrm{a}} + \mathbf{F}^{\mathrm{f}}_{\nu,i} + \sum_{j\neq i} \sum_{\mu\neq\nu} \mathbf{F}^{\mathrm{bb}}_{\nu,i;\mu,j} + \sum_{p} \mathbf{F}^{\mathrm{bs}}_{\nu,i;p} + \mathbf{F}^{\mathrm{r}}_{\nu,i}\,, \tag{7}$$

where $\mathbf{F}^{\mathrm{bb}}_{\nu,i;\mu,j}$ and $\mathbf{F}^{\mathrm{bs}}_{\nu,i;p}$ are the excluded volume force on the ν-th bead in the i-th road due to the bead-bead interaction with the μ-th bead in the j-th rod, and the bead-substrate interaction with the p-th substrate particle, respectively. These pair-wise forces are calculated in LAMMPS using standard neighbour-list algorithms. Moments of total force about the rod centre yield the torque, $\mathbf{T}^{\nu,i}$. The total force and torque on each rod are $\mathbf{F}^{\mathrm{tot}}_i = \sum_\nu \mathbf{F}_{\nu,i}$ and $\mathbf{T}^{\mathrm{tot}}_i = \sum_\nu \mathbf{T}_{\nu,i}$, respectively.

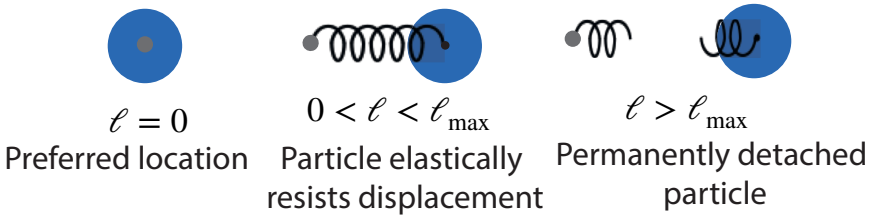

FIG. S1. Three states of a substrate particle in the minimal model of a plastic substrate: (i) Relaxed (ii) Elastic (iii) Plastic.

Substrate particles are single beads that exist on the same two-dimensional plane as the active rods. The equations of motion for the p-th substrate particle are:

$$\frac{d\,\mathbf{r}_p}{dt} = \mathbf{v}_p\,; \quad m_s \frac{d\,\mathbf{v}_p}{dt} = \mathbf{F}^{\mathrm{tot}}_p\,, \tag{8}$$

where m_s is the mass of each substrate particle. The net force $\mathbf{F}_p^{\rm tot}$ on the particle arise due to excluded-volume, elastic and frictional interactions.

- As mentioned above, beads on rods interact with substrate particle through the SSLJ excluded-volume potential, which is described later below. We do not include any direct substrate-substrate excluded-volume interactions.

- Instead, we assume that excluded-volume interactions of substrate particles with each other eventually result in energy being dissipated away over the time-scale over which the semi-solid substrate responds. This effective frictional force on the p-th particle is $\mathbf{F}_p^{\rm f} = -\gamma_s \mathbf{v}_p$ where γ_s is a large substrate friction coefficient.

- In principle, a semi-solid substrate could be modeled by connecting together all particles as a network. To realize faster simulations, a plastic substrate is modeled minimally as follows (Fig. S1). We assume that the position of the substrate particle, $\mathbf{r}_{p,0}$, in its initial, undisturbed, state is its preferred position. On being disturbed to a different position $\mathbf{r}_p$, the particle experiences an elastic restoring force,

$$\mathbf{F}_p^{\rm e} = -\kappa(t)\left(\mathbf{r}_p - \mathbf{r}_{p,0}\right) \ , \ \text{if} \ \mid \left(\mathbf{r}_p - \mathbf{r}_{p,0}\right) \mid < l_{\rm max} \, , \tag{9}$$

  where the stiffness $\kappa(t) = k > 0$ as long as the particle is not disturbed beyond the length, $l_{\rm max}$. As soon as a substrate particle moves beyond this distance, κ is set to zero *i.e.* that particle breaks off permanently, and no longer experiences a restoring force. This mimics the creation of a furrow by bacterial cells by depressing the soft agar permanently [2]. The free substrate particle is still retained in the simulation. Otherwise, if it were to be deleted from the simulation, the frictional resistance from the substrate would continually decrease as furrows form and will eventually vanish completely. Since this is unphysical, free substrate particles are retained in the simulation and offer frictional resistance while being passively advected by the active rods.

- Random thermal forces on the substrate particles are ignored.

The total force on the p-th substrate particle

$$\mathbf{F}_p^{\rm tot} = \mathbf{F}_p^{\rm f} + \mathbf{F}_p^{\rm e} - \sum_i \sum_\nu \mathbf{F}_{\nu,i;p}^{\rm bs} \, , \tag{10}$$

Excluded-volume forces between beads of rods and between beads and substrate particles are calculated using the Separation, Shifted Lennard-Jones (SSLJ) potential [1]. For any two interacting particles, if r is the distance between their centres, then the SSLJ potential is,

$$\phi(r) = \begin{cases} 4\,\epsilon\left[\left(\dfrac{\sigma^2}{r^2+\alpha^2}\right)^6 - \left(\dfrac{\sigma^2}{r^2+\alpha^2}\right)^3\right] - \phi_0, \,, & r \le r_c\,; \\ = 0, \quad r > r_c\,. \end{cases} \tag{11}$$

where σ is the sum of the nominal radii of the interacting particles and r_c is the cut-off distance. We set $r_c = \sigma$. The regularization parameter α ensures that the force is finite when $r = 0$ and, given σ and r_c, it is chosen such that ϕ has a minimum at $r = r_c$. The constant shift ϕ_0 ensures the potential is continuous at $r = r_c$. The softness of the potential is controlled by setting the value of the potential energy, $E = \phi(0)$ when two interacting particles overlap. The energy scale ϵ is then calculated as $\epsilon = \alpha^{12}\,E/(\alpha^{12} - 4\,\sigma^6\,\alpha^6 + 4\sigma^{12})$. We choose E such that the propulsion force on a single rod is insufficient to penetrate into a bead or substrate particle. The penetrability ratio, $Q = LF^{\mathrm{a}}/E$, must hence be low and is set in our simulations to 0.05. The excluded-volume force on the interacting particles is calculated from the spatial gradient of the potential.

Rods of length $L = N_{\mathrm{b}}\,\sigma_{\mathrm{b}}$ are initially arranged as a row at the bottom and top ends of the simulation box of width W and height H. Rods are all initially aligned with the vertical axis. A random packing of 2D spheres is generated using the packages PACKMOL [3] and MOLTEMPLATE [4] to fill the remaining space in the simulation box with substrate particles of nominal diameter $\sigma_{\mathrm{s}} = 0.6\,\sigma_{\mathrm{b}}$. The initial velocities of all rods and substrate particles are set to zero. The polarity vector of each rod is set to point into the simulation box. Bead and substrate particle masses are chosen such that their respective inertial time scales, $m_{\mathrm{b}}/\gamma_{\mathrm{b}}$ and $m_{\mathrm{s}}/\gamma_{\mathrm{s}}$ are much smaller (10^{-4} times) than the diffusive time scale, $\tau_{\mathrm{b}} = \sigma_{\mathrm{b}}^2\,\gamma_{\mathrm{b}}/k_{\mathrm{B}}\,T$. The time-step size Δt is set to be $10^{-5}\,\tau_{\mathrm{b}}$ and is significantly smaller than other physical time scales in the simulation. The values of the magnitude of the propulsion force on a rod, F^{a}, and the elastic stiffness of the substrate particles, k, are decided by the choice of the Péclet number, $\mathrm{Pe} = F^{\mathrm{a}}\,L/k_{\mathrm{B}}\,T$ and the plasticity ratio, $P = k\,l_{\max}/F^{\mathrm{a}}$, for the simulation. Periodic boundary conditions are imposed. Simulations are terminated when any bead reaches the middle of the box at $y = H/2$. The coordinates and velocities of the beads and substrate particles in the top half of the box are reflected about the middle and

are treated as a separate dataset during post-processing. The simulation parameters are summarized in Table S1 below.

TABLE S1. Model parameters

Parameter	**Value**
σ_{b}	1.0
τ_{b}	1.0
$k_{\mathrm{B}}T$	1.0
W	200.0
H	400.0
L	5.0
σ_{s}	0.6
N_{b}	5.0
N_{r}	400
N_{s}	218542
Pe	80,100,150,200
P	0.0025 – 0.075
l_{max}	0.6
m_{b}	10^{-4}
m_{s}	10^{-3}
Δt	10^{-5}

II. FURROW NETWORK MORPHOLOGY

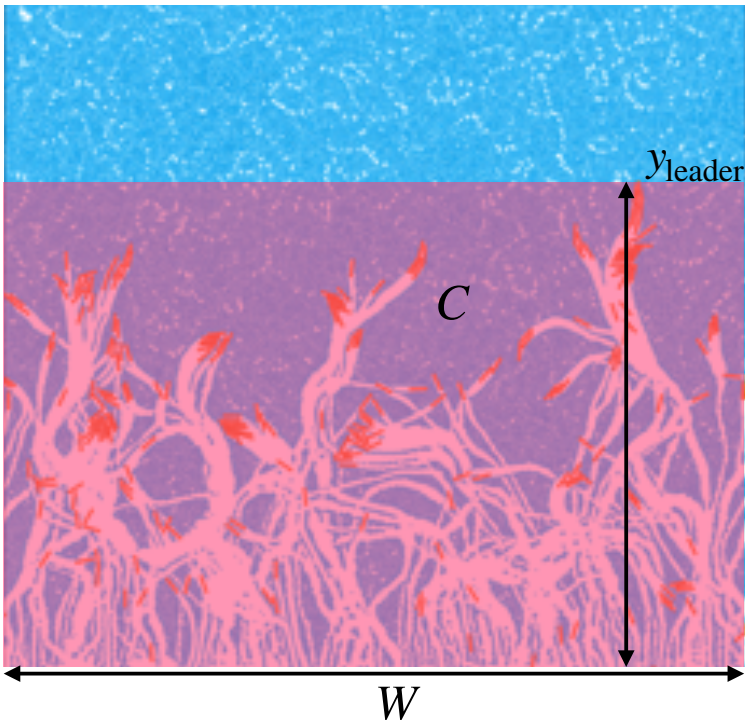

FIG. S2. Colonized area, C, is determined by location of the leader rod.

The colonized area $C(t) = y_{\text{leader}}(t)\,W$, where y_{leader} is the maximum y-coordinate of the centres-of-mass of all the rods in the dataset at any time t (Fig. S2). A list of substrate particles that have been permanently displaced is updated at each time step. The total permanently-furrowed area is equal to the number of these particles multiplied by the area of each substrate particle, $\pi\sigma_{\text{s}}^2/4$. The furrow-substrate interface at the end of a simulation is defined by substrate particles that have not been permanently displaced and are within a distance of σ_{s} from a permanently-displaced particle. To calculate the box-counting fractal dimension, D, of the interface particles, the simulation domain is first divided into a square grid of size, δ, and the number, N_i, of grid elements that contain at least one interface particle is determined. The procedure is repeated for several values of δ. The fractal dimension, D, is then determined as the magnitude of the slope of a straight line fit through the $\log N_i$-versus-$\log \delta$ data.

III. CLUSTER ANALYSIS

Clusters tracking commences only after $C \geq 8LW$. Thereafter, we define a moving *frontier region* as the region with a distance of $8L$ behind y_{leader}. Cluster analysis is carried out for every time step in the frontier region until the simulation ends. At any instant of time, individual clusters are identified by scanning through the inter-bead distance matrix and identifying pairs of beads separated by σ_{b} or less as belonging to the same cluster. Since this assigns all beads belonging to any single rod to the same cluster, the cluster size – defined as the number of rods in a cluster – is the number of beads in a cluster divided by N_{b}.

A contact-neighbour list of rods is generated for each cluster. For each contact neighbour pair, the separation between the centres of mass and relative orientation of contact neighbours, $R_{ij} = |\mathbf{r}_i - \mathbf{r}_j|$ and $Y_{ij} = |\theta_i - \theta_j|$ are calculated, where $\theta_i \in [-\pi, \pi]$ is the polar angle of the orientation vector, $\hat{\mathbf{p}}_i$. If $\mathcal{R}$ and $\mathcal{Y}$ are the sets of contact-neighbour separations and relative orientations, then a cluster is a *train* with rods arranged end-to-end as a line if

$$\min(\mathcal{R}) \geq L \quad \text{AND} \quad \max(\mathcal{Y}) \leq 7^\circ . \tag{12}$$

Any cluster that is not a train is classified as a *raft*. This includes rods with $Y_{ij} \approx \pi$, since such pairs tend to separate from each other. Isolated rods are counted as rafts of unit size.

We calculate the total number of train and raft clusters at each time step and obtain their time-averages, J^{T} and J^{R}, in each simulation run. The fraction of train clusters for that run is, therefore, $f^{\text{T}} = J^{\text{T}}/(J^{\text{T}} + J^{\text{R}})$. Data presented in Fig. 2A of the main paper are the averages of f^{T} over six datasets.

At any time, the orientation angle ϕ of a cluster is the average of the angle made with the vertical axis by member rods in that cluster; that is, the average of $\phi_i = (\pi/2) - \theta_i$. The orientational distributions $p(\phi)$ for trains and rafts in the frontier region is obtained by pooling together cluster data over all time-steps and simulation runs, for a given set of simulation parameters. Orientational distributions are presented in Fig. 2B of the main paper and in Fig. S7 in the Supplementary Results below.

To analyse the speeds of clusters, individual clusters are tracked for the duration of their survival time. A cluster survives intact as long as it has the same members. Each cluster of a unique set of member rods is assigned a unique identifier. The average speed v of a cluster

over its survival time is calculated as the distance travelled by its centre-of-mass divided by its survival time; the average y-component of its velocity, v_y, is its net y-displacement divided by the survival time. The velocity and speed data for all unique clusters across all time-steps and simulation runs are pooled together for trains and rafts. We calculate size-wise and overall averages of v and v_y. The overall averages are presented in Fig. 2C of the main paper. The size-wise averages are presented in Fig. S5 in the Supplementary Results below.

IV. SUPPLEMENTARY RESULTS

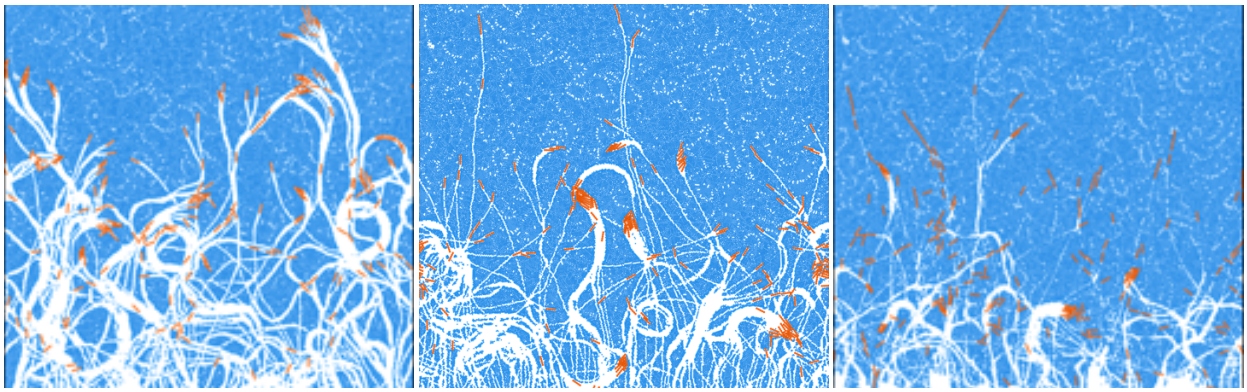

FIG. S3. Colony morphology at simulation termination with Pe = 100 and P = 0.0025 (left), P = 0.025 (centre), P = 0.075 (right): substrate particles are blue, active rods are red, and the white regions devoid of substrate particles are furrows. At small P (left) most of the clusters in the frontier region are rafts while at high P(right), clusters are mostly trains.

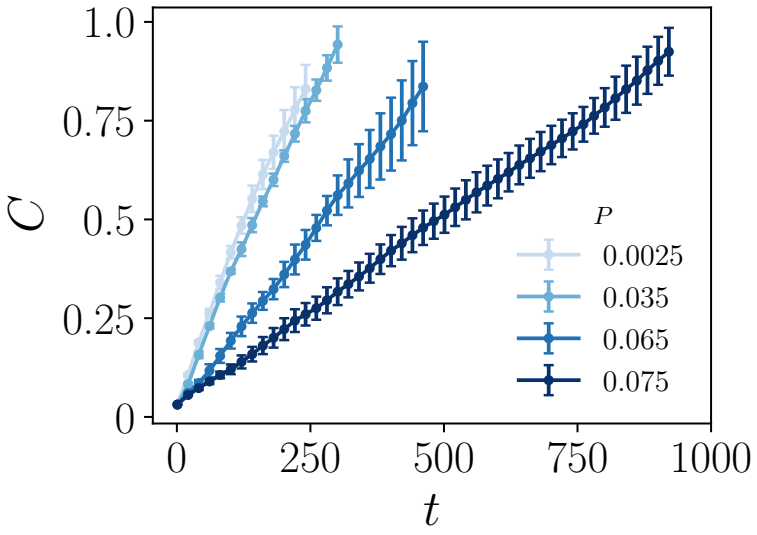

FIG. S4. Growth of colonized area, C, at Pe = 100. The colonized area increases nearly linearly over the duration of the simulations.

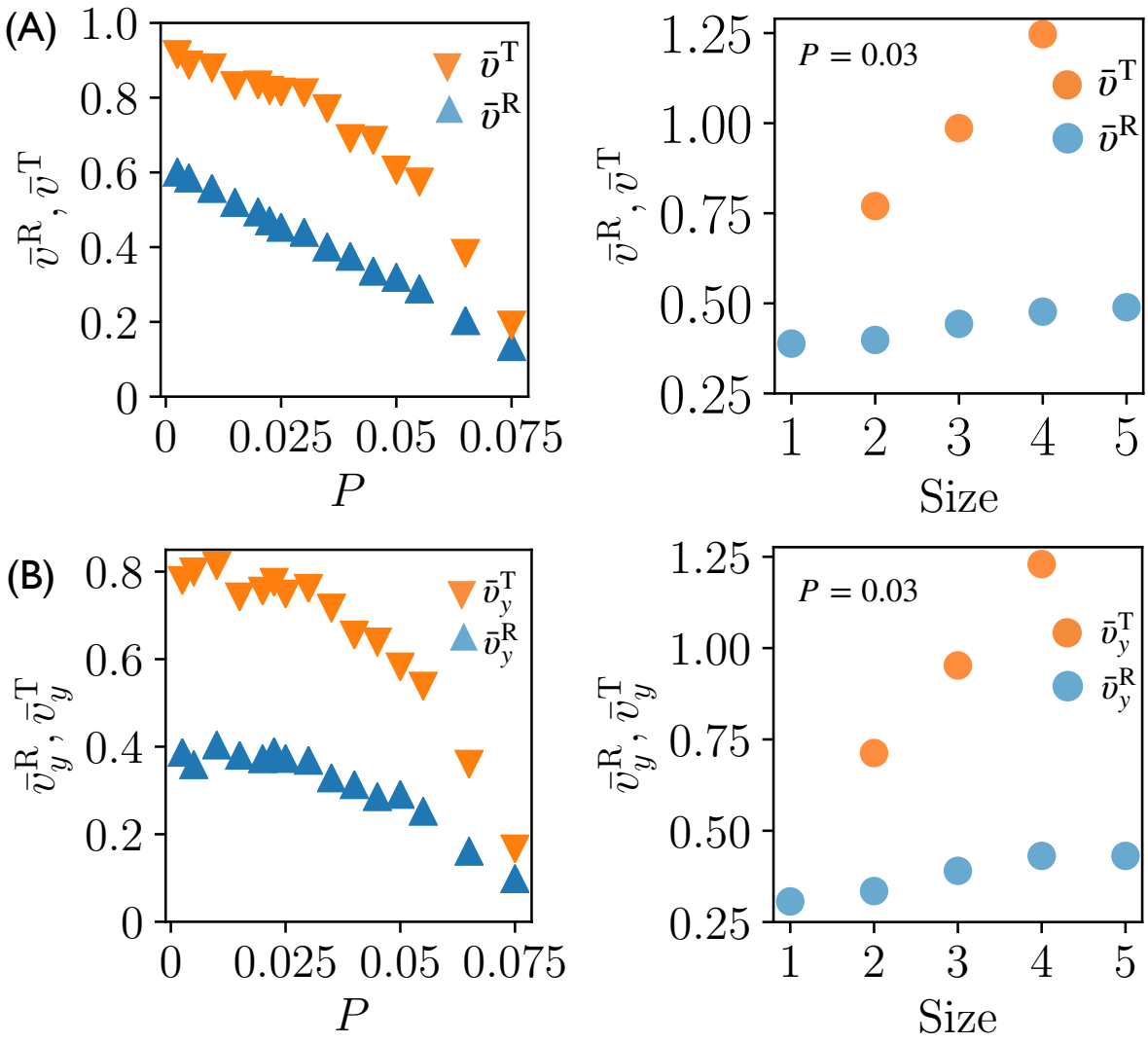

FIG. S5. Dependence of (A) average cluster speed and (B) average y-component of cluster velocity on substrate plasticity (left) and cluster size, for (i) trains (orange) and (ii) rafts (blue), at Pe = 100.

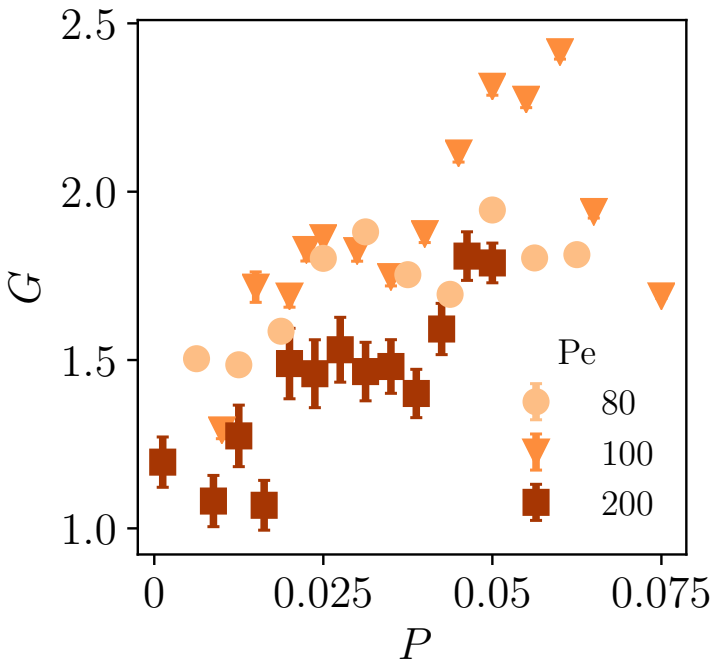

FIG. S6. Speed gain, $G = V_c/V_1$, ratio of the colonization speed and speed of single isolated rod through substrate.

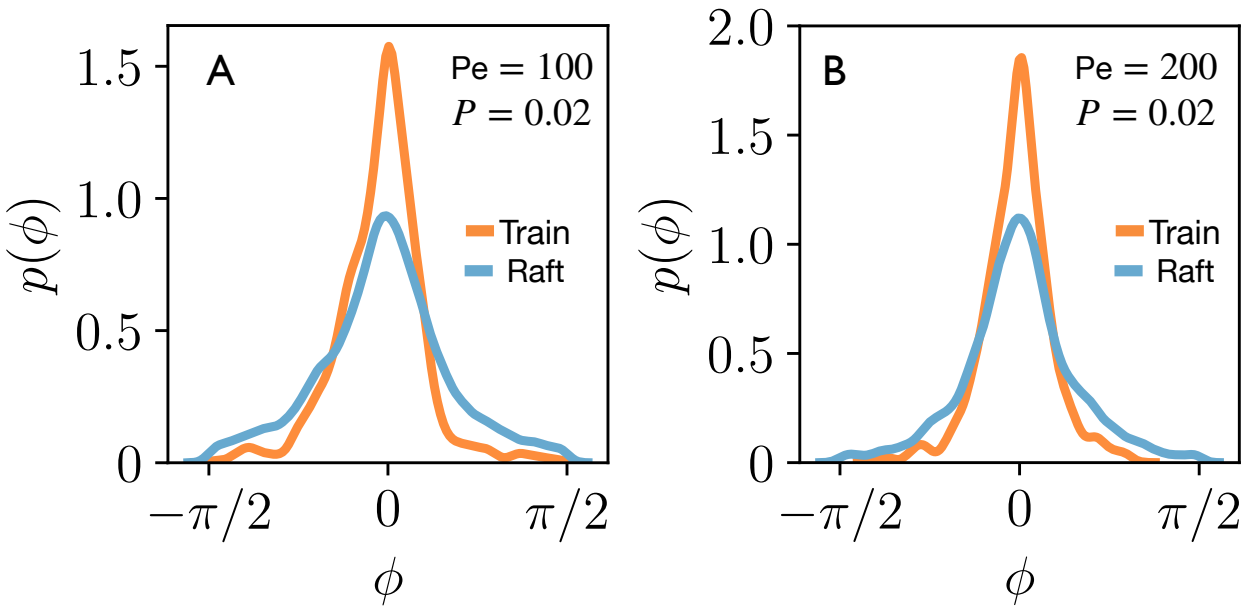

FIG. S7. Normalized frequency distribution of rod orientation angle , ϕ with respect to the vertical axis (y axis).

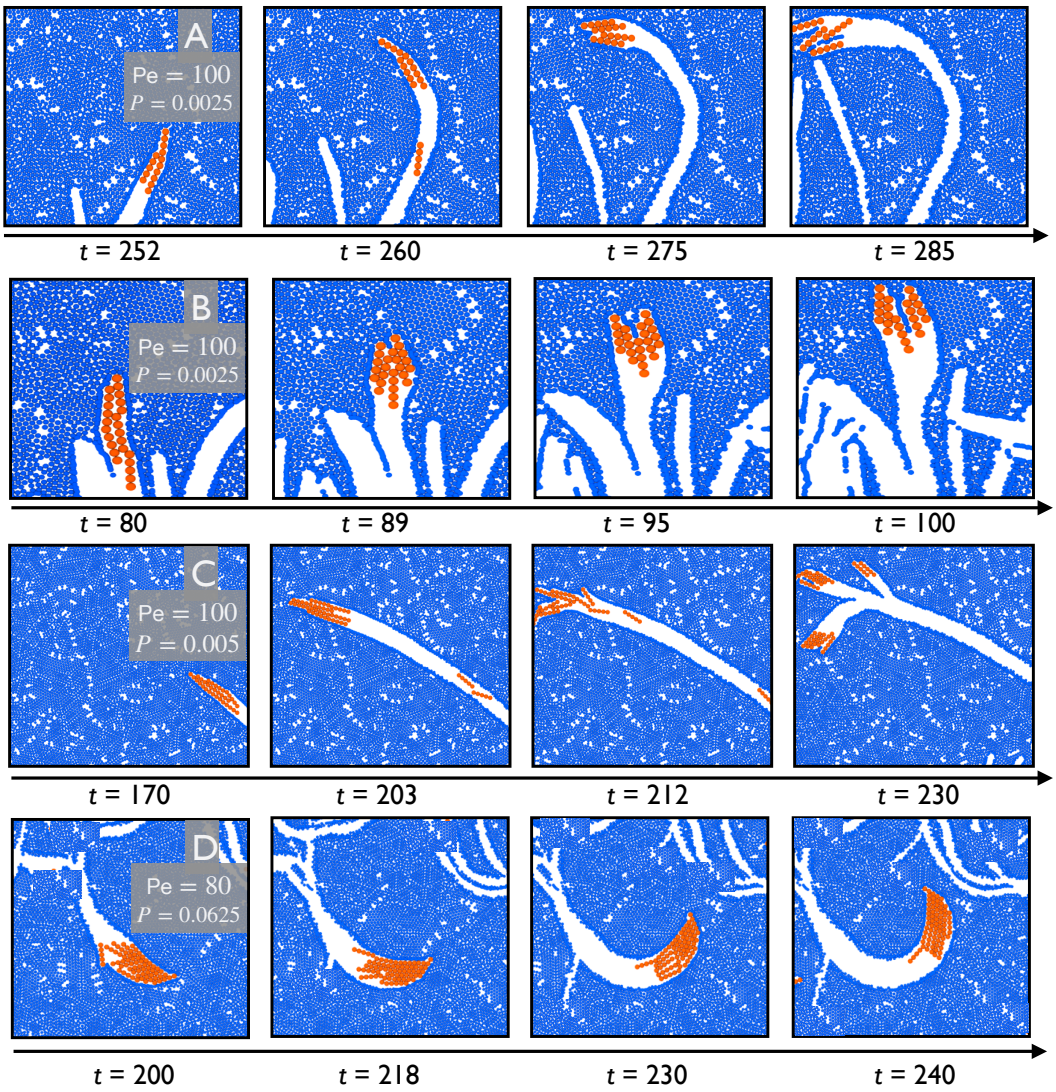

FIG. S8. Examples of breakup of stable pointy raft clusters. (The arrow at the bottom of each panel represents that the figures should be read from left to right). (A) A free rod moving up through an empty furrow collides with a pointy raft to create an unstable flat cluster head (Pe = $100, P = 0.0025$). (B) Rods within a pointy raft slide past each other to catch up with the head of the raft, creating an unstable flat cluster head (Pe = $100, P = 0.0025$). (C) Collisions with multiple free rods from the rear perturbs orientation of rods in the pointy raft to break it up into smaller rafts (Pe = $100, P = 0.005$). (D) A large pointy raft creating a wide, curved furrow (Pe = $80, P = 0.0125$).

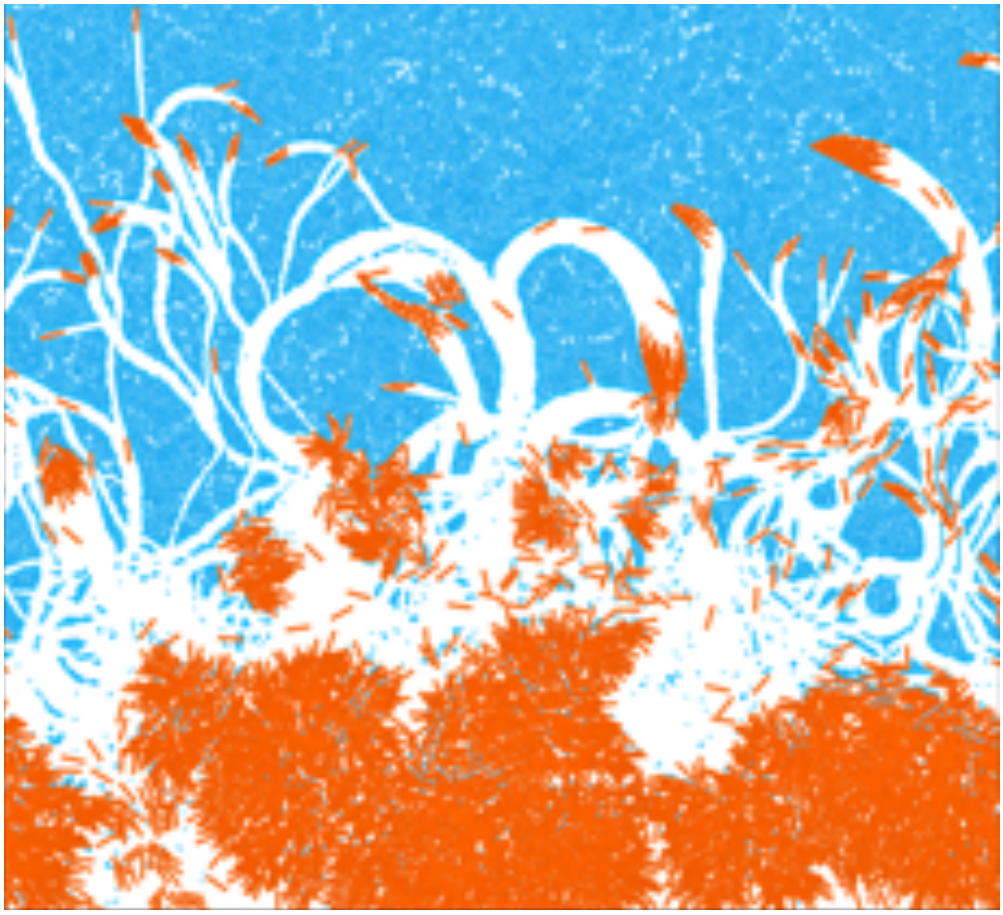

FIG. S9. Colony morphology at Pe = 100 and P = 0.0025, with linear rod influx in the system. Rods are introduced at a linear rate of 25 rods per τ_b.

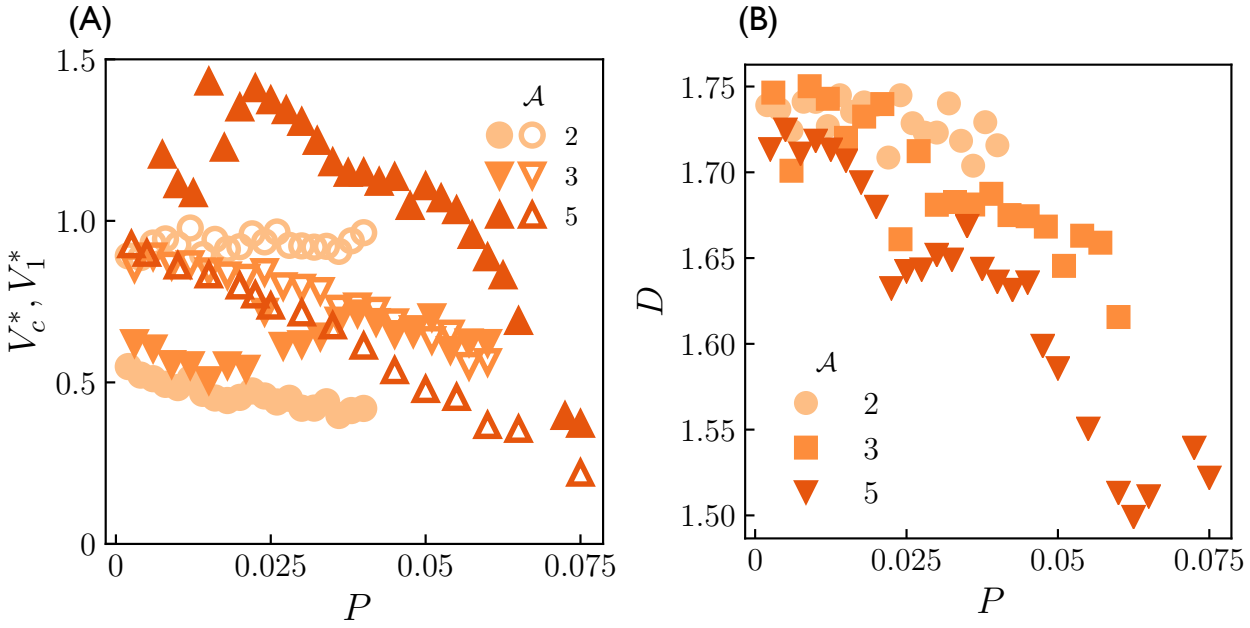

FIG. S10. Effect of rod aspect ratio, $\mathcal{A}$, on (A) Comparison of normalised colonisation speed, V_c^* (filled symbols), and the normalised speed of isolated rods, V_1^* (open symbols) and (B) Box-counting fractal dimension as a function of plasticity number P, measured at termination of simulation.

The rod aspect ratio, $\mathcal{A}$ (= N_b), does have a significant influence on the colonization rate and the morphology of the furrow network. Figure S10 presents results showing the influence of rod aspect ratio. With $\mathcal{A}$ = 2, the colonization rate, V_c, decreases monotonically with substrate plasticity, without the distinct peak at a non-zero plasticity (Fig. S10 A). The colonization rate, V_c, is smaller than the isolated-rod *speed* trough the substrate, V_1. This is due to the fact that V_c is related to the average y-component of the low-aspect ratio particles, whereas V_1 is the speed. While small raft-like clusters do form, collective effects are not strong enough to provide the strong enhancement of V_c observed with $\mathcal{A}$ = 5. This appears consistent with the results of Peruani et al. [5] for free rods, that, at any given Pe, large clusters become rarer as the aspect ratio decrease. With $\mathcal{A}$ = 3, we observe a small peak in the colonization rate as P is increased, accompanied by a transition from rafts to trains along (not shown). Aspect ratio also influences colony morphology. The small clusters with $\mathcal{A}$ = 2 lead to the emergence of a more dense furrow network with fractal dimension closer to 2 than that of the network obtained with $\mathcal{A}$ = 5 at the same relative substrate plasticity, P (Fig. S10 B).

V. MOVIES

Movies have been generated using the OVITO software [6].

Movie §1: Colonisation at $P = 0.0125$) and Pe = 100: active rods initially form individual furrows and subsequently form clusters.

Movie §2: Dominance of train clusters at high substrate stiffness ($P = 0.075$, Pe = 100).

Movie §3: Motion and breakup of a large raft cluster (yellow; $P = 0.0125$, Pe = 100). The cluster cuts through previous narrow furrow networks unhindered, but "evaporates" in a larger furrow when its members have freedom to escape into the furrow network.

Movie §4: Collision of a single rod with a cluster leads to break up of the cluster; this corresponds to Fig. S8-A.

Movie §5: Fluctuation of rods' orientation within a cluster leads to break-up of cluster; this corresponds to Fig. S8-B.

Movie §6: Collision of multiple rods with a cluster leads to break up of the cluster; this corresponds to Fig. S8-C.

Movie §7: Formation of wide furrow network by a large pointy raft; this corresponds to Fig. S8-D.

Movie §8: Steady influx of new active rods at the box boundary leads to formation of large clusters behind the frontier that destroy the furrow network created by the vanguard clusters; this corresponds to Fig S9.

Movie §9: Comparison of morphology formed by random initial condition and aligned rod initial condition at $P = 0.0125$) and Pe = 100.

---

[1] Masoud Abkenar, Kristian Marx, Thorsten Auth, and Gerhard Gompper. Collective behavior of penetrable self-propelled rods in two dimensions. *Physical Review E*, 88(6):062314, 2013.

[2] Erin S Gloag, Lynne Turnbull, Alan Huang, Pascal Vallotton, Huabin Wang, Laura M Nolan, Lisa Mililli, Cameron Hunt, Jing Lu, Sarah R Osvath, et al. Self-organization of bacterial biofilms is facilitated by extracellular dna. *Proceedings of the National Academy of Sciences*, 110(28):11541–11546, 2013.

[3] Leandro Martínez, Ricardo Andrade, Ernesto G. Birgin, and José Mario Martínez. Packmol: A package for building initial configurations for molecular dynamics simulations. *Journal of Computational Chemistry*, 30(13):2157–2164, 2009. URL `http://dblp.uni-trier.de/db/journals/jcc/jcc30.html#MartinezABM09`.

[4] Andrew I Jewett, David Stelter, Jason Lambert, Shyam M Saladi, Otello M Roscioni, Matteo Ricci, Ludovic Autin, Martina Maritan, Saeed M Bashusqeh, Tom Keyes, et al. Moltemplate: A tool for coarse-grained modeling of complex biological matter and soft condensed matter physics. *Journal of molecular biology*, 433(11):166841, 2021.

[5] Fernando Peruani, Andreas Deutsch, and Markus Bär. Nonequilibrium clustering of self-propelled rods. *Physical Review E*, 74(3):030904, 2006.

[6] Alexander Stukowski. Visualization and analysis of atomistic simulation data with OVITO-the Open Visualization Tool. *Modelling and Simulation in Materials Science and Engineering*, 18, 2010.